Proceedings of the ASME 2010 3rd Joint US-European Fluids Engineering Summer Meeting and 8th International Conference on Nanochannels, Microchannels, and Minichannels
FEDSM-ICNMM2010
August 1-5, 2010, Montreal, Canada

FEDSM-ICNMM2010-30781

TIME DOMAIN MODELS FOR DAMPING-CONTROLLED FLUIDELASTIC INSTABILITY FORCES IN MULTI-SPAN TUBES WITH LOOSE SUPPORTS

Marwan Hassan *
Mechanical Engineering Department
University of New Brunswick
Fredericton, New Brunswick, Canada
Email: hassanm@unb.ca

Robert Rogers
Mechanical Engineering Department
University of New Brunswick
Fredericton, New Brunswick, Canada
Email: rjr@unb.ca

Andrew Gerber
Mechanical Engineering Department
University of New Brunswick
Fredericton, New Brunswick, Canada
Email: agerber@unb.ca

ABSTRACT

This paper presents simulations of a loosely supported multi-span tube subjected to turbulence and fluidelastic instability forces. Several time-domain fluid force models simulating the damping controlled fluidelastic instability mechanism in tube arrays are presented. These models include the negative damping model based on the Connors equation, fluid force coefficient-based models (Chen; Tanaka and Takahara), and two semi-analytical models (Price and Païdoussis; and Lever and Weaver). Time domain modelling challenges for each of these theories are discussed. The implemented models are validated against available experimental data. The linear simulations show that the Connors-equation based model exhibits the most conservative prediction of the critical flow velocity when the recommended design values for the Connors equation are used.

The models are then utilized to simulate the nonlinear response of a three-span cantilever tube in a lattice bar support subjected to air crossflow. The tube is subjected to a single-phase flow passing over one of the tubes spans and the flow velocity and the support clearance are varied. Special attention is paid to the tube/support interaction parameters that affect wear, such as impact forces, contact ratio, and normal work rate. As was seen for the linear cases, the reduced flow velocity at the instability threshold differs for the fluid force models considered. The investigated models do, however, exhibit similar response characteristics for the impact force, tip lift response, and work rate, except for the Connors-based model that overestimates the response and the tube/support interaction parameters for the loose support case, especially at large clearances.

NOMENCLATURE

U	Flow velocity.
U_c	Critical flow velocity.
d	Tube diameter.
f_n	Natural frequency.
f	Vibration frequency.
K	Connors constant.
$F_L(t)$	Fluid lift force.
$F_D(t)$	Fluid drag force.
y_L	Tube lift displacement.
y_D	Tube drag displacement.
α, σ, τ and β	Fluid added-mass coefficients.
α', σ', τ' and β'	Fluid-damping coefficients.
α'', σ'', τ'' and β''	Fluid-stiffness coefficients.
δ	Structural damping logarithmic decrement.
ρ	Fluid density.

INTRODUCTION

The structural integrity of tube bundles represents a major concern when dealing with high risk industries such as nuclear steam generators where the rupture of a tube or tubes will lead to the undesired mixing of the primary and secondary fluids. Flow-induced vibration is one of the major concerns that could lead to compromising the structural integrity. The tubes are therefore

*Address all correspondence to this author.

stiffened by means of supports to avoid these vibrations. To accommodate the thermal expansion of the tube, as well as to facilitate the installation of these tube bundles, clearances are allowed between the tubes and their supports. As the clearances between the tubes and their supports become larger due to progressive tube wear or chemical cleaning, the tube/support impact and rubbing may become more frequent and severe. These increased impacts can lead to tube damage due to fatigue and/or wear at the support locations. The economic consequences of this type of failure have resulted in a considerable amount of research devoted to understanding the excitation mechanisms leading to such damage, which include turbulent buffeting, vortex shedding, fluidelastic instability (FEI), and acoustic resonance [1, 2].

Among these mechanisms, fluidelastic instability has the potential to induce large vibration amplitudes when the critical flow velocity (U_c) is exceeded, which may cause catastrophic failures. As such, a great deal of research was initiated to develop empirical models and design guidelines for fluidelastic instability [3–6]. In addition, a number of theoretical models have been developed that have also contributed to understanding the phenomenon [7–11]. A summary of the knowledge and a description of the available theoretical models can be found in the work of Price [12]. As well, a critical examination of these models with respect to their contributions and deficiencies can be found in a recent paper by Weaver [13]. Using these FEI models, the safe operating flow velocity (U) can be selected such that U/U_c does not exceed an appropriate factor of safety.

Alternatively, proper design of the tube geometry and the locations of the supports could mitigate the risk of fluidelastic instability. Such designs assumes prior knowledge of the tube vibratory behaviour. This usually implies that each tube is considered to be simply supported at the support locations (linear support conditions). This is a reasonable assumption if the tube/support clearance is small. However, the linear assumption can be quite misleading when clearances are large. It is argued that for loosely-supported tubes, unstable modes may develop at much lower flow velocities than the stability threshold. This may lead to higher tube/support impacts which in turn may result in unacceptable levels of wear. Au-Yang [14] showed that precritical fluidelastic forces were responsible for the unacceptable tube wear in several operating steam generators. Therefore, estimation of the fluidelastic forces in tube bundles is an important step towards a successful evaluation of the fretting wear. The available FEI models and empirical formulae [7–11] are merely utilized to predict the linear critical flow velocity. In addition, very limited attempts to develop time-domain models suitable for wear predictions have been reported. This requires formulations that express the response amplitude resulting from FEI. With this goal in mind, previous attempts were made to extend the capability of the original FEI models in order to account for temporal behaviour [15–19].

This paper [1] presents modelling and implementation of several time domain FEI force models. These models are adaptations of the conventional linear FEI models within the framework of a finite element model of tubes with loose supports. INDAP (Incremental Nonlinear Dynamic Analysis Program), which is in an in-house finite element code [20], is utilized to test the numerical modelling challenges associated with each model. The paper also attempts to address two important questions: 1) What is the effect of loose supports on the the stability threshold? and 2) What is the resulting tube/support interaction parameters in the subcritical region (flow velocities below the critical flow velocity).

TUBE TIME-DOMAIN EQUATION

The equation of motion of a tube subjected to crossflow including intermittent contact, can be written as:

$$[M]\left\{\ddot{y}\right\}+[C]\left\{\dot{y}\right\}+[K]\left\{y\right\}=\left\{F_t(t)\right\} + \left\{F_f(\ddot{y},\dot{y},y,t)\right\}+\left\{F_{imp}(\dot{y},y,t)\right\} \tag{1}$$

where M, C and K are the structural mass. stiffness and damping matrices, respectively. F_t represents the known external turbulence force vector. F_f is the fluidelastic instability force vector, which contains the drag and the lift components (F_D and F_L). F_{imp} is the impact force vector that includes all normal contact (F_c) and friction forces (F_{fr}) due to all supports. Equation 1 is discretized via beam finite elements and integrated via the Newmark method with a modal superposition approach [21].

FLUIDELASTIC INSTABILITY MODELLING

Fluidelastic instabilities can be categorized as damping-controlled instability and stiffness-controlled instability. A combination of the two mechanisms exists in most cases with damping controlled instability being dominant for low mass-damping parameters. The available approaches for time-domain modelling of fluidelastic instability are summarized below. Detailed descriptions of these time-domain models can be found in [22]. The treatment of fluidelastic instability will be approached here by utilizing the damping-controlled instability only.

Quasi-static model

The quasi-static model was originally developed by considering multiple tubes moving synchronously such that the net work done on a tube could result in having a component of the

[1] An early version of this paper was presented at the 6th Canadian Nuclear Society's International Steam Generator Conference, Toronto, Nov., 2009.

lift force in phase with the tube velocity. Several empirical design guidelines based on Connors-type equations have been developed. For a tube array with d being the tube diameter, f_n the structural natural frequency, m the tube mass per unit length, δ the structural damping logarithmic decrement, and ρ the fluid density, the critical pitch flow velocity (U_c) is expressed as:

$$\frac{U_c}{f_n d} = K\left(\frac{m\delta}{\rho d^2}\right)^a \tag{2}$$

K and a are empirical constants which were originally proposed for a tube row by Connors [8] to be 9.9 and 0.5, respectively. The above expression represents a very simple relationship between reduced flow velocity ($U_r = \frac{U}{fd}$) and the mass-damping parameter ($K\left(\frac{m\delta}{\rho d^2}\right)^a$). With the assumption that Connors equation accurately models the physics of fluidelastic instability, numerous investigations were carried out to find the appropriate value of Connors constant. This also resulted in several modifications of the original equation to fit the experimental data for tube arrays. In turn, a more complex expression than the original Connors equation emerged. Price [23] and Weaver [13] examined the contributions and validity of this model. They concluded that there is little scientific justification for using Connors equation, or variations to predict the critical flow velocity. However, because of its simplicity, this equation became the industry standard for design of tube bundles against fluidelastic stability mechanism. Although the original quasi-static model in its original form was developed for multiple tube rows (more than one tube is required for instability to occur), an equivalent velocity-dependent damping ratio was introduced to account for FEI in the nonlinear simulations [15]:

$$\xi = \xi_o\left[1 - \frac{f}{f_n}\left(\frac{U}{U_c}\right)^2\right] \tag{3}$$

where ξ is the net damping ratio including the effect of FEI, while ξ_o is the damping ratio in quiescent liquid. The critical flow velocity U_c and the vibration frequency f are required to utilize the above equation. Ignoring the frequency effect would result in errors in the estimated tube/support interaction parameters.

Alternatively, an equivalent damping-controlled destabilizing force is used here. The fluid destabilizing lift force per unit length (F_L) can be expressed in the form of a time-dependent force equivalent to Connors' equation as follows [17]:

$$F_L = \frac{8\pi^2\rho U^2 \dot{y}_L}{fK^2} \tag{4}$$

where $\dot{y}_L$ is the tube lift velocity and U is the pitch flow velocity. This expression enables the implementation of non-uniform flow distribution along the tube length.

Unsteady flow model

In the unsteady flow model, the fluid forces $(F_L,\ F_D)$ acting on a tube within a tube array are a function of the tube lift and drag displacements $(y_L,\ y_D)$, velocity $(\dot{y}_L,\ \dot{y}_D)$, acceleration $(\ddot{y}_L,\ \ddot{y}_D)$ and the corresponding values of the neighbouring tubes. The motion-dependent fluid forces acting on a single flexible tube are expressed as follows [7]:

$$F_L = -\frac{\rho\pi d^2}{4}(\alpha_{11}\ddot{y}_L + \sigma_{11}\ddot{y}_D) + \frac{2\pi\rho U^2}{f}(\alpha'_{11}\dot{y}_L + \sigma'_{11}\dot{y}_D) + \rho U^2(\alpha''_{11}y_L + \sigma''_{11}y_D) \tag{5}$$

$$F_D = -\frac{\rho\pi d^2}{4}(\tau_{11}\ddot{y}_L + \beta_{11}\ddot{y}_D) + \frac{2\pi\rho U^2}{f}(\tau'_{11}\dot{y}_L + \beta'_{11}\dot{y}_D) + \rho U^2(\tau''_{11}y_L + \beta''_{11}y_D) \tag{6}$$

α, σ, τ and β are the added mass coefficients. α', σ', τ' and β' are the fluid-damping coefficients. α'', σ'',τ'' and β'' are the fluid-stiffness coefficients. These fluid force coefficients can be obtained experimentally (see Tanaka and Takahara [9] and Chen [7]) or numerically as shown in a recent work (see Omar et al. [24]).

Quasi-steady flow model

Based on the Price and Païdoussis model [11], the fluidelastic instability forces acting on a tube are expressed in terms of the tube motion through the lift and drag coefficients. No assumption, such as harmonic motion, is made. The fluidelastic force derived from this model is expressed explicitly in the real motion of the tube in the following form:

$$F_L = \frac{\rho d U^2}{2a^2}\left[\frac{\partial C_L}{\partial \bar{y}}y_L(t-\tau) - \frac{d}{U}C_D\dot{y}_L(t)\right] \tag{7}$$

where a is the reduced pitch $\left(a = \frac{P}{P-d}\right)$, $\frac{\partial C_L}{\partial y}$ is the rate of lift coefficient, C_D is the drag coefficient, and τ is a time lag. The model was later transformed into the so-called 'quasi-unsteady' model [25] in which a better representation of the time lag was presented. The representation of time lag required several parameters to be determined experimentally. Later, Meskell [26] presented a numerical model for estimating the quasi-unsteady parameters. In this work, the original time lag expression will be utilized.

Flow redistribution model

In its original form, the flow redistribution model of Lever and Weaver [10] idealizes the tube as a single degree of freedom system vibrating at its natural frequency. Briefly, the fluid is assumed to flow through a series of flow channels passing between the tubes. The flow inside each channel is assumed to be one dimensional and incompressible, and the fluidelastic excitation is independent of wake phenomena. The motion of the single flexible tube in a rigid array causes the dimensions of the flow channel to change. This change in the flow channel's dimensions is postulated to lag behind the tube motion, which in turn leads to unsteadiness in the flow. A pressure perturbation that lags behind the tube motion will also be produced. The resultant fluid forces will have a component in-phase with the tube velocity.

As mentioned earlier, for response computation in the presence of loose supports, it is necessary to calculate the external fluid forces in terms of the tube response. Hassan and Hayder [19] reformulated this model to account for any arbitrary motion in the time domain, making it suitable for implementation within the finite element framework. The flow is discretized axially into a number of flow cells where each flow cell contains two flow channels. Each channel has a length of s_o and a cross sectional area of A, as shown in Fig. 1. For each flow channel, the pressure at any point along the moving tube/channel interface is calculated by solving both the unsteady continuity and the momentum equations. The pressure is integrated along this tube/channel contact area to obtain the lift and the drag force per unit length ($F_L(t)$ and $F_D(t)$). The channel dimensions, channel/tube contact length and perturbation time lag can be obtained from the tube geometry and array pitch-to-diameter ratio [19].

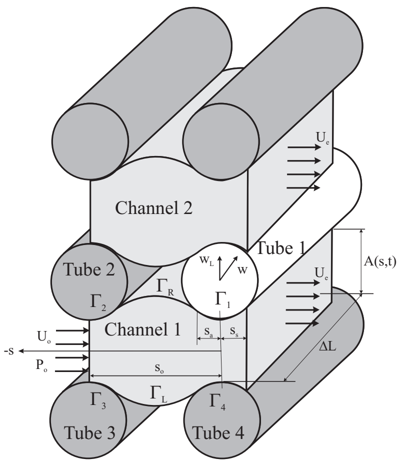

FIGURE 1. Flow channels concept for tube arrays (Lever and Weaver [27]).

TUBE AND SUPPORT MODELLING

The mathematical modelling of the tube/support impact has been described in detail and verified by Hassan et al. [21]. Briefly, the tube is discretized into beam finite elements and the proper boundary conditions are applied. Any loose support configuration can be modelled by a number of mass-less bars arranged around the tube. Each bar is attached by an equivalent contact spring and damper (Fig. 2). If the normal component of the tube displacement (y_n) exceeds the radial support clearance (C_r), contact takes place. The normal contact forces are calculated in each bar by evaluating the elastic ($K_c(y_n - C_r)$) and damping $C_c\dot{y}_n$ forces in the spring and the damper. K_c and C_c are the spring stiffness and the damping coefficient, respectively, where $C_c = 1.5\alpha K_c(y_n - C_r)$ is proportional to the the elastic contact force. The force balance friction model [28] was used to compute the shear contact forces. More details on the modelling and selection of the support parameters and friction modelling can be found in the works of Rogers and Pick [29], Tan and Rogers [30], Hassan et al. [21], and Hassan and Rogers [28].

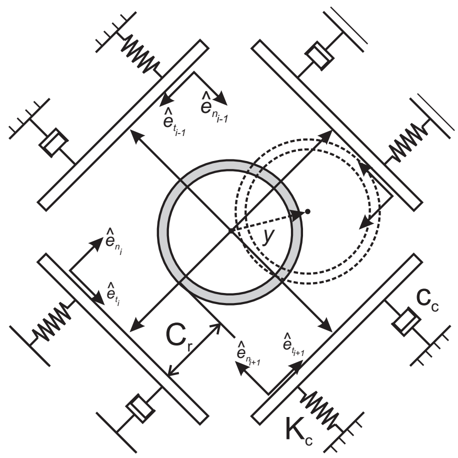

FIGURE 2. Tube/support modelling.

TURBULENCE MODELLING

Fluid excitation due to turbulence is modelled as randomly distributed forces. To implement this approach, the empirically based bounding spectrum of turbulence excitation is obtained using the flow velocity, the tubes diameter, and the array geometry. Several bounding spectra have been proposed (Oengören and Ziada [31]; Taylor and Pettigrew [32]), which can be used to generate the random excitation forces. The PSD curve is then transformed into a force-time record using an inverse Fourier transform algorithm. The resulting fluctuating forces are Gaussian in nature with a zero mean value. For each flow velocity, two different force versus time records are created for each velocity region representing the fluid excitation in the lift and the drag directions. These force-time records are fully uncorrelated.

TUBE MODEL

The tube geometry used for this work is shown in Fig. 3. The geometry and flow structure were adapted from Vincent et al. [33] and was chosen based on the use of four clearance supports and the reversing flow within each channel. The tube bundle is normal triangular with a pitch-to-diameter ratio of 1.35. The constant parameters for the simulations are listed in Table 1. INDAP [21] software was used to run the nonlinear transient dynamic simulations. The supports were taken as rhomboid flat-bar supports. The tube was subjected to both turbulence and fluidelastic excitation. Details on how to select the values of the constant parameters and the sensitivity of the resulting contact forces can be found in [21, 29]. Cross flow is assumed to be distributed along the tube as shown in Fig. 3. For each case study, ten seconds of response time history were computed. The tube/support interaction response parameters were averaged over the simulation time record, excluding an initial transient period. Response details will be presented for two radial clearance values (0.1 mm and 0.4 mm).

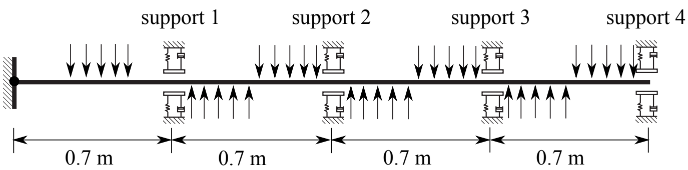

FIGURE 3. Tube model.

Parameter	Value
Outside diameter	12.7 mm
Inside diameter	11 mm
Material	Inconel 600
Modulus of elasticity	199.8 GPa
Poisson's ratio	0.28
Support stiffness	1.0 MN/m
Support damping	0.25 s/m
Friction coefficient	0.2
Modal damping ratio	0.005
Tube density	8304 kg/m^3
Outside fluid density	5.38 kg/m^3
Inside fluid density	803.1 kg/m^3
No. of elements	84
Element length	0.0333 m

TABLE 1. Simulation parameters

RESULTS

Linear Simulations

Numerical investigations with no clearance were first carried out and compared with published experimental data [4]. A number of simulations were conducted where the velocity was incremented until instability was attained. To simulate fluidelastic instability using the Connors equation, the empirical constant has to be selected. A value of $K = 3$ recommended by the ASME Boiler Code [34] is utilized throughout this work. The Price and Païdoussis model requires knowing the tube lift and drag fluid-force coefficients. For this array geometry, lift-force coefficient rate and drag fluid-force coefficients (C_D) are -19.2 and 3.8, respectively [11]. In addition, the time lag parameter (τ) is set as $\frac{d}{U}$.

As pointed out earlier, the added stiffness and the damping coefficients for the lift and drag directions are required to utilize Chen's model. For this purpose force coefficient data for $P/d = 1.35$ was obtained numerically by Omar et al. [24].

Fig. 4 shows the force coefficient data employed with Chens model. Using computational fluid dynamics a single tube is oscillated, in the lift and drag directions, at a fixed frequency. Forces are monitored on the centre and surrounding tubes, and further processed by FFT to obtain the amplitude and phase information for the motion dependent forces. The coefficients presented in Fig. 4 reflect a subset of these motion dependent forces. An important aspect in this approach is that both lift and drag forces are included (Eqs. 5 and 6) and no empirical constants need to be adjusted. Significant computational resources do however need to be deployed in computing the coefficients, and care needs to be taken in applying boundary conditions and appropriate physical model assumptions [24].

When utilizing the Lever and Weaver model [10], the flow attachment and separation angles, relevant fluid length parameter and required channel dimensions are set in accordance with their recommended parameter values in [10]. The channel perturbation time lag is a very important parameter, which affects the quality of the predicted threshold. This parameter is dependent on the selection of the relevant fluid length (l_o). In the original model, the relevant fluid length was select intuitively as $L_o = 2s_o$ (baseline value). Andjelic and Popp [35] recommended modified values for the relevant fluid length to achieve acceptable agreement with their experimental stability thresholds for normal triangle array. Hassan and Hayder [19] conducted an investigation of the effect of the variation of the relevant fluid length on the nonlinear response. They found minor effects on the lift response when the fluid length was increased by 200% of the baseline value. In the absence of a better guidance; the base line value will be utilized in all nonlinear simulations reported in this paper.

When utilizing the Connors-based and Chen-based equations, the vibration frequency is required. Because of the loose supports, the vibrations frequency is not known a priori. Several methods can be utilized to obtain the vibration frequency [16–18, 36]. In this work, the zero-crossing frequency method is utilized. In addition to being frequency-dependent, the fluid force coefficients required for the Chen-based equations are functions of Reynolds number. Therefore, for each simulated flow velocity the fluid force coefficients are interpolated from the values at Fig. 4. Expressing the fluid force in the semi-analytical models [10, 11] in terms of the current and past displacements represents an advantage since the current vibration frequency is not required.

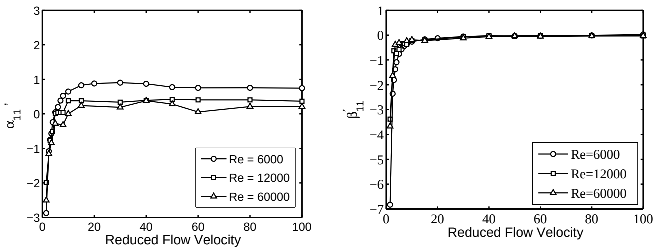

(a) (b)

FIGURE 4. Fluid force coefficients for P/d=1.35 [24]: (a) α'_{11}; (b) β'_{11}.

Fig. 5 shows the predicted critical flow velocities using the proposed time domain models with linear supports and the experimental stability data reported from the literature. Only the experimental data with values of pitch-diameter ratio close to 1.35 were compared to the present numerical investigations. It is shown in Fig. 5 that the FEI models predict different stability thresholds. Connors model using the recommended ASME design value ($K = 3$) resulted in a lower bound prediction ($U_{cr} = 4.5$). On the other hand the prediction of the Price and Païdoussis model represents an upper bound ($U_{cr} = 29$). The linear simulation results of the Chen ($U_{cr} = 14$) and the Lever-Weaver ($U_{cr} = 20$) models agree well with the available experimental data.

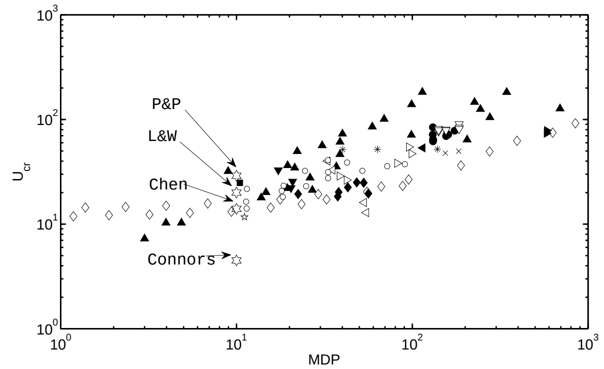

FIGURE 5. Comparison of the predicted linear critical flow velocity with the experimental data for the normal triangle array case: ○ Austermann and Popp [37], ⋆ Andjelic and Popp [35], ⧫ Connors [38], ▲ Price and Zahn [39], ◇ Teh and Goyder [40], ∗ Weaver and Yeung [41], × Scott [42], ► Elkashlan [43], ▼ Gorman [44], ▷ Zukauskas and Kathinas [45], ◁ Chen and Jendrzejczyk [46], ◄ Gross [47], • Hartlen [48], ▽ Pettigrew et al. [49], − Simulations

Nonlinear Simulations

For the supports with clearance, the tube was assumed to be perfectly aligned in the supports initially. For each support clearance, a number of reduced flow velocities $U_r = U/f_n d$ were simulated covering the linear stability thresholds of the first unconstrained mode, the first constrained modes, and up to the nonlinear instability. The reduced flow velocity was calculated using the natural frequency of the lowest linearly supported mode. Fig. 6 shows samples of the tube displacement response spectra at a point near the fixed end support, using the Lever and Weaver model for four reduced flow velocities (1.2, 4.9, 14.7, 21.9). For a reduced flow velocity of 1.2, the tube response is low, such that very few impacts occur between the tube and the supports. The response spectrum is dominated peaks at frequencies that correspond to the unconstrained natural frequencies of the tube (Fig. 6a). Increasing the reduced flow velocity to 4.9 results in an increase in both the drag and the lift response such that frequent impact takes place. The corresponding response spectrum shows the evolution of higher modes and a significant increase in the vibration frequency (Fig. 6b). A further increase in the flow velocity ($U_r = 14.7$) results in a higher drag and lift response and the response spectra becomes rather noisy with no dominant peaks (Fig. 6c). As the flow velocity approaches the stability threshold of the linear system, the response is dominated by a frequency that corresponds to the fundamental frequency of the lowest constrained mode (Fig. 6d).

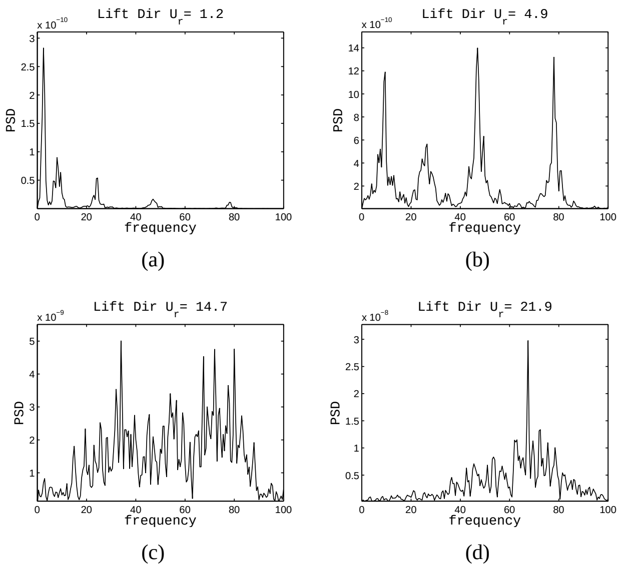

FIGURE 6. Response spectra for 0.4 mm clearance case: Reduced flow velocity (a) 1.2; (b) 4.9; (c) 14.7; (d) 21.9.

The rms lift response of the middle of the third span for the 0.1 mm radial clearance case is shown in Fig. 7a. The lift response is almost independent of the flow velocity for the lower range of reduced flow velocity (up to U_r = 15). The lift response increases at a larger rate beyond a reduced flow velocity of 20. The nonlinear instability threshold for the Connors, Chen, Lever-Weaver, Price-Païdoussis models were observed at reduced flow velocities of 8, 24.5, 50, and 61, respectively. These velocities are higher than those of the linear instability values (4.5, 14, 20, and 29). The increase in the nonlinear instability threshold can be attributed to increase in damping due to the friction at the supports. However, the increase is not constant for all models. For example the delay in instability due to support damping (expressed as the percentage increase in the nonlinear stability threshold) is 80%, 57%, 150%, and 110%, respectively. Similar trends were observed for the 0.4 mm radial clearance case (Fig. 7b). Table 2 summerieses the predicted linear and nonlinear stability threshold. For all models, the lift response is larger than that of the 0.1mm clearance case for the range of reduced flow velocities up to 30. The nonlinear stability thresholds also occurred at approximately the same reduced flow velocities.

Fig. 8 shows the rms normal-direction impact force as a function of the reduced flow velocity. The results show that the impact force due to the support contacting the third support

Model	Linear	Nonlinear ($C_r = 0.1$ mm)	No linear ($C_r = 0.4$ mm)
Connors	4.5	8.1	8.3
Chen	14	22	24.5
L & W	20	50	50
P & P	29	61	61

TABLE 2. Stability threshold $(U_{cr} = \frac{U_c}{f_n d})$

pair increases as the flow velocity increases (Fig. 8a). The response is mainly controlled by the turbulence excitation for the pre-instability region which results in similar values predicted by the four models. However, when approaching instability large impact force levels are observed. Connors model predicts a higher level of impact force, especially for the large clearance case $(C_r = 0.4$ $mm)$ as shown in Fig. 8b. Work rate is calculated by averaging the product of the impact forces and the tube sliding displacement over the sampling time. Fig. 9a shows the predicted work rate as a function of the reduced flow velocity. In general, the highest work rate is predicted using the Connors model (Fig. 9b). The prediction of work rate utilizing the Lever-Weaver model and Price-Païdoussis models yielded similar results.

CONCLUSION

Several time domain fluidelastic instability force models were presented. Using these models, simulations of the damping-controlled fluidelastic instability mechanism in tube arrays were conducted. Numerical investigations of the response of a single flexible loosely-supported tube within a rigid array subjected to cross-flow were carried out. All the models predicted stability thresholds of the loosely-supported tube that are higher than those of the linearly-supported tube. The greatest difference in the predictions can be attributed to both the level of drag response and the amount of damping as a function of the flow velocity. Tube response was found to increase as the radial clearance increased. Increasing the radial clearance also resulted in a delay in the stability threshold. In addition, clearance seems to have little effect on the predicted impact force level up to the critical flow velocity. However, a larger work rate is observed for larger clearances, especially for the Connors model.

ACKNOWLEDGMENT

The authors would like to thank the Natural Sciences and Engineering Research Council of Canada for funding this research project.

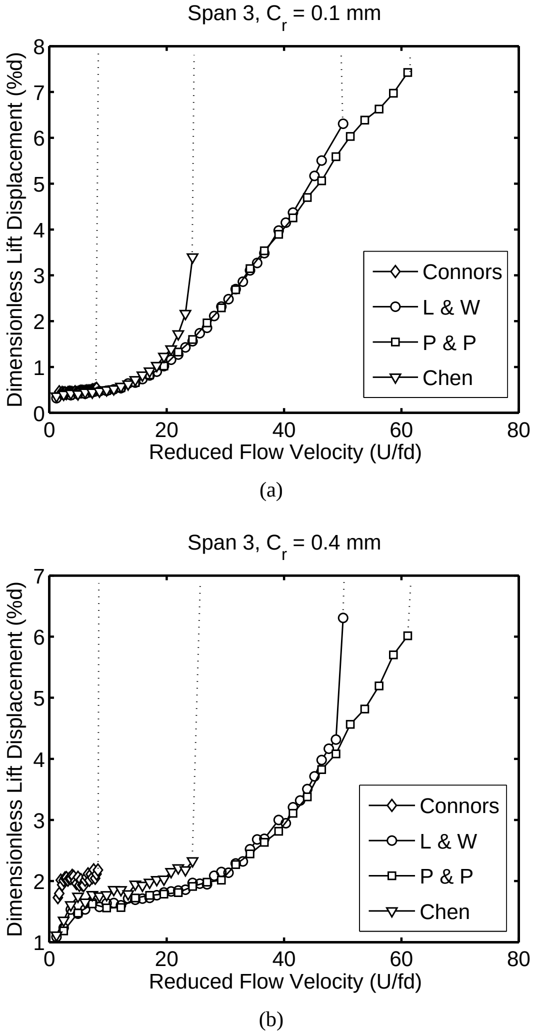

FIGURE 7. Lift response vs. reduced flow velocity for span 3:(a) C_r = 0.1 mm; (b) C_r = 0.4 mm.

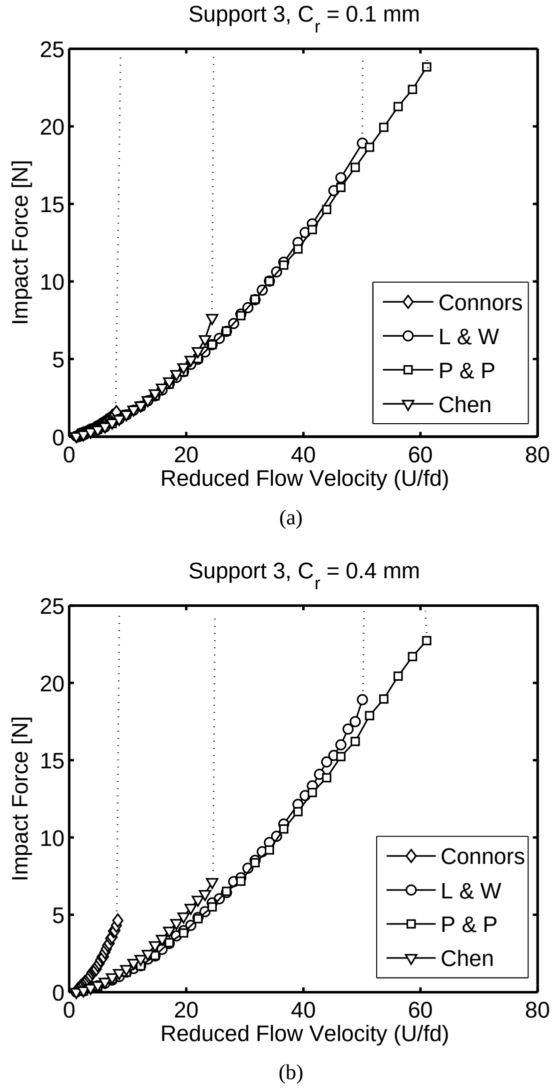

FIGURE 8. Impact force vs. reduced flow velocity for support 3: (a) C_r = 0.1 mm; (b) C_r = 0.4 mm.

REFERENCES

[1] Weaver, D., Ziada, S., Au-Yang, M., Chen, S., Païdoussis, M. P., and Pettigrew, M., 2000. "Flow-induced vibrations in power and process plant components - progress and prospects". *Journal of Pressure Vessel Technology, Transactions of the ASME*, ***122***, pp. 339–348.

[2] Pettigrew, M., and Taylor, C., 2003. "Vibration analysis of steam generators and heat exchangers : An overview part 1: Flow damping, fluidelastic instability". *Journal of Fluids and Structures*, ***18***(5), pp. 469–483.

[3] Chen, S., S., 1984. "Guidelines for the instability flow velocity of tube arrays in cross-flow". *Journal of sound and Vibrations*, ***93***, pp. 439–455.

[4] Weaver, D., and Fitzpatrick, J., 1988. "A review of cross-flow induced vibrations in heat exchanger tube arrays". *Journal of Fluids and Structures*, ***2***, pp. 73–93.

[5] Pettigrew, M., and Taylor, C., 1991. "Fluidelastic instability of heat exchanger tube bundles. review and design recommendations". *Journal of Pressure Vessel Technology, Transactions of the ASME*, ***113***(2), May, pp. 242–256.

[6] Schröder, K., and Gelbe, H., 1999. "New design recommendations for fluidelastic instability in heat exchanger tube bundles". *Journal of Fluids and Structures*, ***13***, pp. 361–379.

[7] Chen, S., 1983. "Instability mechanisms and stability criteria of a group of circular cylinders subjected to cross-flow. part 1: theory". *Journal of Vibration, Acoustics, Stress, and*

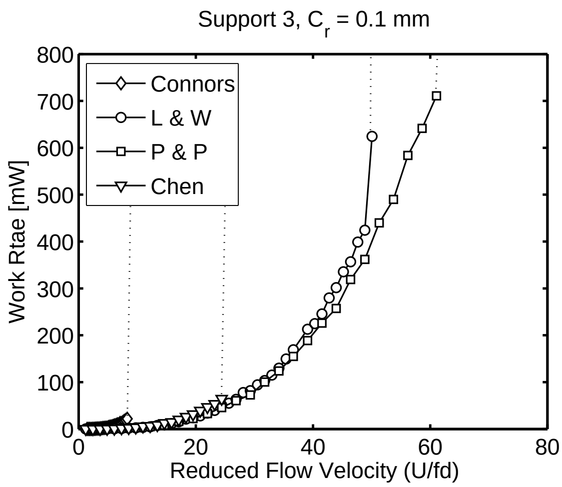

(a)

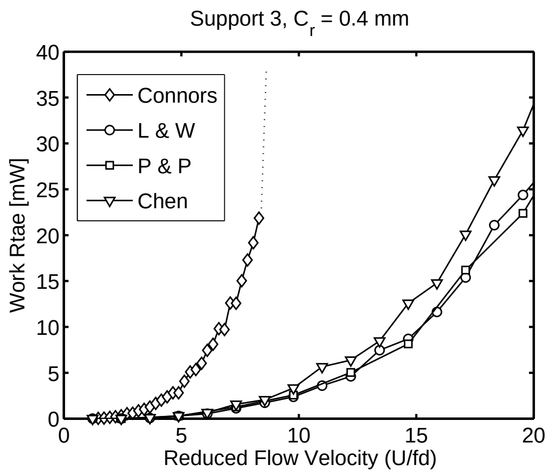

(b)

FIGURE 9. Work rate vs. reduced flow velocity for support 3: (a) C_r = 0.1 mm; (b) C_r = 0.4 mm.

Reliability in Design, ***105***, pp. 51–58.

[8] Connors, H. J., 1970. "Fluidelastic vibration of tube arrays excited by cross flow". In Flow-Induced Vibration in Heat Exchangers, D. D. Reiff, ed., ASME, pp. 42–57.

[9] Tanaka, H., and Takahara, S., 1981. "Fluid elastic vibration of tube array in cross-flow". *Journal of Sound and Vibration*, ***77***, pp. 19–37.

[10] Lever, J. H., and Weaver, D. S., 1982. "A theoretical model for the fluidelastic instability in heat exchanger tube bundles". In Flow-Induced Vibration of Circular Cylindrical Structures, S. S. Chen, M. P. Païdoussis, and M. K. Au-Yang, eds., pp. 87–108.

[11] Price, S. J., and Païdoussis, M. P., 1984. "An improved mathematical model for the stability of cylinder rows subjected to cross-flow". *Journal of Sound and Vibration*, ***97***(4), pp. 615–640.

[12] Price, S. J., 1995. "A review of theoretical models for fluidelastic instability of cylinder arrays in cross-flow". *Journal of Fluids and Structures*, ***9***, pp. 463–518.

[13] Weaver, D. S., 2008. "Some thoughts on the elusive mechanism of fluidelastic instability in heat exchanger tube arrays". In The 9th International Conference on Flow-Induced Vibration.

[14] Au-Yang, M. K., 1987. "Flow-induced wear in steam generator tubes prediction versus operational experience". In Flow Induced Vibration and Noise, Vol. 53-2, ASME, pp. 265 – 273.

[15] Axisa, F., Antunes, J., and Villard, B., 1988. "Overview of numerical methods for predicting flow-induced vibration". *Journal of Pressure Vessel Technology, Transactions of the ASME*, ***110***, pp. 6–14.

[16] Fricker, A., 1992. "Numerical analysis of the fluid-elastic vibration of a steam generator tube with loose support". *Journal of Fluids and Structures*, ***6***, pp. 85–107.

[17] Sauvé, R., 1996. "A computational time domain approach to fluidelastic instability for nonlinear tube dynamics". In ASME PVP/ICPVT-8 Conference on Symposium on Flow Induced Vibrations, M. Pettigrew, ed., ASME, pp. 111–121.

[18] Eisinger, F., Rao, M., Steininger, D., and Haslinger, K., 1995. "Numerical simulation of cross-flow induced fluidelastic vibration of tube arrays and comparison with experimental results". *Journal of Pressure Vessel Technology*, ***111***, pp. 378–384.

[19] Hassan, M., and Hayder, M., 2008. "Modelling of fluidelastic vibrations of heat exchanger tubes with loose supports". *Nuclear Engineering and Design*, ***238***(10), pp. 2507 – 2520.

[20] Dokainish, M., 1988. *Incremental Nonlinear Dynamic Analysis Program: User's Manual*. McMaster University, Canada.

[21] Hassan, M., Weaver, D., and Dokainish, M., 2002. "A simulation of the turbulence response of heat exchanger tubes in lattice-bar supports". *Journal of Fluids and Structures*, ***16***(8), pp. 1145–1176.

[22] Hassan, M., and Achraf, H., 2009. "Time domain models for damping-controlled fluidelastic instability forces in tubes with loose supports". In ASME Symposium on Flow Induced Vibrations.

[23] Price, S. J., 2001. "An investigation on the use of connors' equation to predict fluidelastic instability in cylinder arrays". *Journal of Pressure vessel Technology*, ***123***, pp. 448 – 453.

[24] Omar, H., Hassan, M., and Gerber, A., 2009. "Numerical estimation of fluidelastic instability in staggered tube ar-

rays". In ASME Symposium on Flow Induced Vibrations.
[25] Granger, S., and Païdoussis, M. P., 1996. "An improvement to the quasi-steady model with application to cross-flow-induced vibration of tube array". *Journal of Fluid Mechanics*, ***320***, pp. 163–184.
[26] Gillen, S., and Meskell, C., 2008. "Variation of fluidelastic critical velocity with mass ratio and reynolds number in a densely packed normal triangular tube array". In Flow Induced Vibrations, I. Zolotarev and J. Horáêek, eds., pp. 193–198.
[27] Lever, J. H., and Weaver, D. S., 1982. "A theoretical model for the fluidelastic instability in heat exchanger tube bundles". *Journal of Pressure Vessel Technology, Transactions of the ASME*, ***104***, pp. 104–147.
[28] Hassan, A., and Rogers, R., 2004. "Friction modelling of preloaded tube contact dynamics". In The 8th International Conference on Flow-Induced Vibration, E. De Langre and F. Axisa, eds., pp. 295–300.
[29] Rogers, R., and Pick, R., 1977. "Factors associated with support plate forces due to heat exchanger tube vibratory contact". *Nuclear Engineering and Design*, ***44***(2), pp. 247–253.
[30] Tan, X., and Rogers, R. J., 1998. "Simulation of friction in multi-degree-of-freedom vibration systems". *ASME Journal of Dynamic Systems, Measurement, and Control*, ***120***, pp. 144–146.
[31] Oengören, A., and Ziada, S., 2000. "Flow periodicity and acoustic resonance in parallel triangle tube bundles". *Journal of Fluids and Structures*, ***14***(2), pp. 197–219.
[32] Taylor, C. E., and Pettigrew, M. J., 2000. "Random excitation forces in heat exchanger tube bundles". *Journal of Pressure Vessel Technology*, ***122***, pp. 509–514.
[33] Vincent, M., Hassan, M., and Rogers, R., 2009. "A probabilistic assessment technique applied to a cracked heat exchanger tube subjected to flow-induced vibration". *Journal of pressure vessel technology*, ***131***(3), pp. 031305.1–031305.6.
[34] Au-Yang, M., 2001. *Flow-Induced Vibration of Power and Process Plant Components - A Practical Workbook*. ASME Press.
[35] Andjelíc, M., and Popp, K., 1989. "Stability effects in a normal triangular cylinder array". *Journal of Fluids and Structures*, ***3***(2), Mar., pp. 165–185.
[36] Au-Yang, M. K., 2002. "The crossing frequency as a measure of heat exchanger support-plate effectiveness". *Journal of Fluids and Structures*, ***16***, pp. 83–92.
[37] Austermann, R., and Popp, K., 1995. "Stability behaviour of a single flexible cylinder in rigid tube arrays of different geometry subjected to cross-flow". *Journal of Fluids and Structures*, ***9***(3), pp. 303 – 322.
[38] Connors, H. J., 1980. "Fluidelastic vibration of tube arrays excited by nonuniform cross flow". In Flow-Induced Vibration of Power Plant Components, Publication PVP, Vol. 41, pp. 93–107.
[39] Price, S. J., and Zahn, M. L., 1991. "Fluidelastic behaviour of a normal triangular array subject to cross-flow". *Journal of Fluids and Structures*, ***5***, pp. 259 – 278.
[40] Teh, C. E., and Goyder, H. G. D., 1988. "Data for the fluidelastic instability of heat exchanger tube bundles". In Symposium on Flow Induced Vibration and Noise, M. P. Païdoussis, S. S. Chen, and M. D. Bernstein, eds., Vol. 3, pp. 77–94.
[41] Weaver, D. S., and Yeung, H. C., 1984. "The effect of tube mass on the flow induced response of various tube arrays in water.". *Journal of Sound and Vibration*, ***93***, pp. 409–425.
[42] Scott, P., 1987. "Flow visualization of cross-flow-induced vibrations in tube arrays". Master's thesis, McMaster University, Hamilton, Ontario, Canada.
[43] Elkashlan, M., 1983. "Array geometry effects on vortex shedding and instability in heat exchanger tube array". PhD thesis, McMaster University, Ontario, Canada.
[44] Gorman, D., 1976. "Experimental development of design criteria to limit liquid cross-flow induced vibration in nuclear reactor heat exchanger equipment". *Nuclear Science and Engineering*, ***61***, pp. 324–336.
[45] Zukauskas, A., and Katinas, V., 1980. "Flow-induced vibration in heat-exchanger tube banks. in practical experiences with flow-induced vibrations (eds e. naudascher and d. rockwell)". pp. 188–196.
[46] Chen, S. S., and Jendrzjczyk, J. A., 1981. "Experiments on fluid instability in tube banks subjected to liquid cross flow". *Journal of Sound and Vibration*, ***78***, pp. 355–381.
[47] Gross, H., 1975. "Untersuchung aeroelastischer schwingungsmechanismen und deren berucksichtigung bei der auslegung von rohrbundelwarmetauschern". PhD thesis, Technical University of Hannover.
[48] Hartlen, R. T., 1974. Wind tunnel determination of fluidelastic vibration thresholds for typical heat-exchanger tube patterns. Report No. 74-309-K. Ontario Hydro Research Division.
[49] Pettigrew, M., and Gorman, D., 1978. "Vibration of heat exchanger components in liquid and two-phase cross-flow". In Proceedings BNES International Conference on Vibration in Nuclear Plant.